MOLECULAR AND CELLULAR BIOLOGY, Oct. 2005, p. 8531–8540 Vol. 25, No. 19
0270-7306/05/$08.00+0 doi:10.1128/MCB.25.19.8531–8540.2005

The BTB-kelch Protein KLHL6 Is Involved in B-Lymphocyte Antigen Receptor Signaling and Germinal Center Formation†

Jens Kroll,[1]¶‡ Xiaozhong Shi,[1]¶ Arianna Caprioli,[1]¶ Hong-Hsing Liu,[1]¶
Claudia Waskow,[4] Keng-Mean Lin,[3] Toru Miyazaki,[2]
Hans-Reimer Rodewald,[4] and Thomas N. Sato[1,5]*

Departments of Internal Medicine and Molecular Biology,[1] Center for Immunology,[2] and Alliance for Cellular Signaling and Department of Pharmacology,[3] University of Texas Southwestern Medical Center at Dallas, Dallas, Texas 75390; Department of Immunology, University of Ulm, D-89070 Ulm, Germany[4]; and Department of Cell and Developmental Biology, Weill Medical College of Cornell University, New York, New York 10021[5]

Received 4 December 2005/Returned for modification 27 January 2005/Accepted 7 July 2005

BTB-kelch proteins can elicit diverse biological functions but very little is known about the physiological role of these proteins in vivo. Kelch-like protein 6 (KLHL6) is a BTB-kelch protein with a lymphoid tissue-restricted expression pattern. In the B-lymphocyte lineage, KLHL6 is expressed throughout ontogeny, and KLHL6 expression is strongly upregulated in germinal center (GC) B cells. To analyze the role of KLHL6 in vivo, we have generated mouse mutants of KLHL6. Development of pro- and pre-B cells was normal but numbers of subsequent stages, transitional 1 and 2, and mature B cells were reduced in KLHL6-deficient mice. The antigen-dependent GC reaction was blunted (smaller GCs, reduced B-cell expansion, and reduced memory antibody response) in the absence of KLHL6. Comparison of mutants with global loss of KLHL6 to mutants lacking KLHL6 specifically in B cells demonstrated a B-cell-intrinsic requirement for KLHL6 expression. Finally, B-cell antigen receptor (BCR) cross-linking was less sensitive in KLHL6-deficient B cells compared to wild-type B cells as measured by proliferation, Ca^{2+} response, and activation of phospholipase Cγ2. Our results strongly point to a role for KLHL6 in BCR signal transduction and formation of the full germinal center response.

BTB-kelch proteins possess two distinct domains: BTB (for *B*road-Complex, *T*ramtrack and *B*ric a brac) and kelch domains (1). The first member of the BTB-kelch family, termed Kelch, was recognized in *Drosophila melanogaster*, where it was required for stabilizing F-actin fibers in the egg chamber (32). This F-actin stabilization function of *Drosophila* Kelch was mediated, in part, by the Src signaling pathway (13). Since the first recognition of *Drosophila* Kelch, more proteins of this family have been identified (1). However, many of these newly identified BTB-kelch proteins have only been characterized in vitro. These studies suggested roles for BTB-kelch proteins in a variety of cell biological processes, such as stabilization/remodeling of cytoskeletons and cell migration (1). Most recently, it has also been shown that many of the BTB proteins (including the ones that also possess the kelch domain) serve as a substrate-specific adapter for cullin 3 ubiquitin ligases (8, 19, 31).

In contrast to these in vitro data, very little is known about the physiological functions of BTB-kelch proteins in vivo, particularly in mammals. The most extensively studied mammalian BTB-kelch is Keap1 (12). Keap1 interacts with the transcription factor Nrf2, which regulates the expression of downstream genes encoding detoxifying and antioxidant proteins (12). Deletion of the *Keap1* gene in mice results in the constitutive activation of Nrf2 and postnatal lethality (30). Another mammalian BTB-kelch protein whose in vivo function has been studied is Kelch homolog 10 (KLHL10) (33). Haploinsufficiency of this gene in mice causes infertility (33). The third mammalian BTB-kelch gene known to have an important physiological function is gigaxonin, which is mutated in giant axon neuropathy (2, 29). Our bioinformatics analysis of the human and mouse genomes has identified at least 38 and 42 BTB-kelch proteins, respectively (H.-H. Liu and T. N. Sato, unpublished). The function of most of these BTB-kelch proteins is unknown.

We have isolated a BTB-kelch protein, KLHL6, by virtue of its expression in embryonic but not adult endothelial cells (see below). The same gene was recently shown to be highly expressed in sheep Peyer's patch and human tonsil B cells (9). Based on this specific expression pattern in adult mice, it has been suggested that KLHL6 might be involved in B-cell functions, notably the germinal center reaction (9). Here, we describe B-cell compartments and B-cell functions in constitutive and conditional KLHL6-deficient mice. While early stages of B-cell development were unaffected, the loss of KLHL6 expression leads to reduced numbers of mature B cells. Antigen-dependent germinal center formation and B-cell antigen receptor (BCR) signaling were impaired in mice lacking KLHL6. Thus, in this report we establish a role for a BTB-Kelch protein in BCR signal transduction and germinal center formation.

* Corresponding author. Mailing address: Department of Cell and Developmental Biology, Weill Medical College of Cornell University, Box 60, 1300 York Avenue, New York, NY 10021. Phone: 212-746-6013. Fax: 212-746-9017. E-mail: island1005@aol.com.

† Supplemental material for this article may be found at http://mcb.asm.org.

¶ These four authors contributed equally to this work.

‡ Present address: Tumor Biology Center, Freiburg i.Br., Germany.

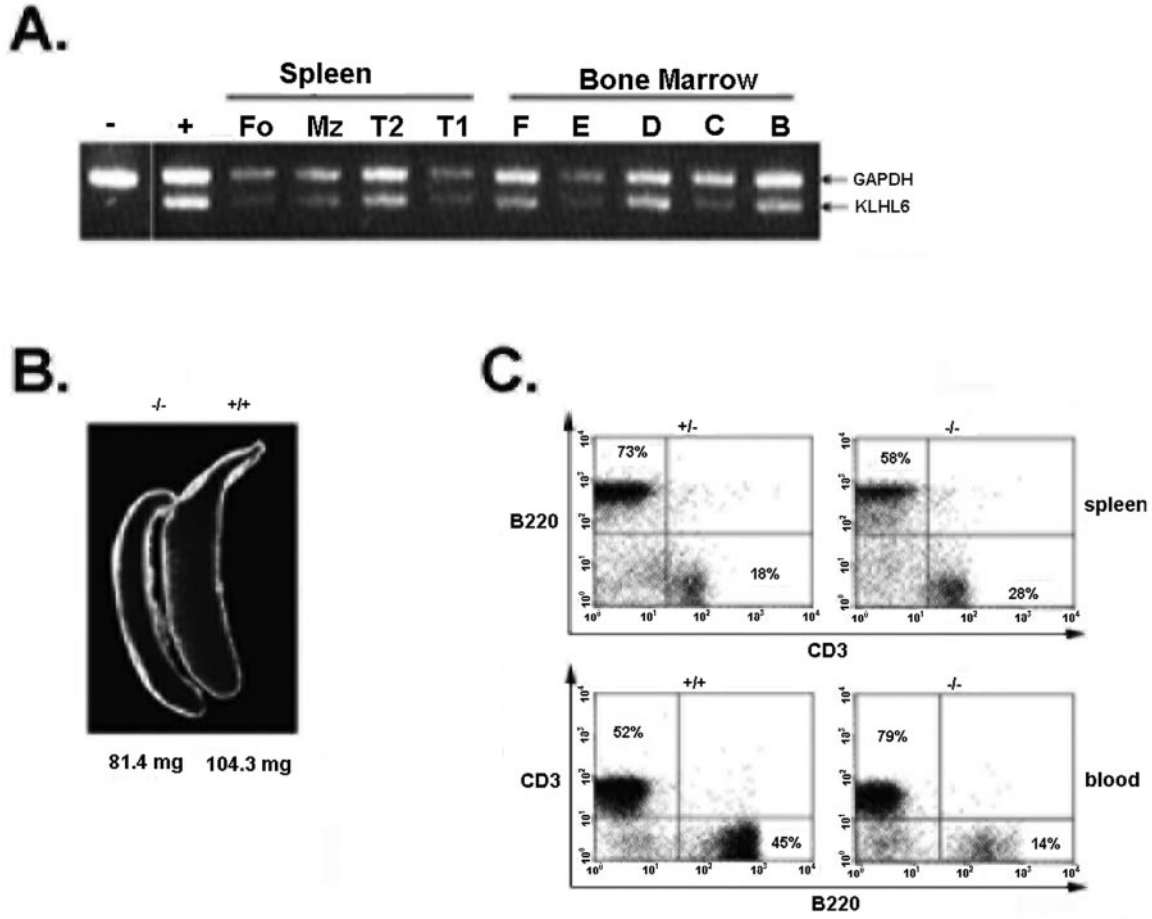

FIG. 1. Expression of KLHL6 in B lymphocytes, and effect of loss of KLHL6 on peripheral B cells. (A) Analysis of KLHL6 mRNA expression by RT-PCR in a broad range of immature and mature B-lymphocyte subpopulations in bone marrow and spleen. Bone marrow cells were sorted into fractions B ($B220^+$ $CD43^+$ $CD24^+$ $BP\text{-}1^-$), C ($B220^+$ $CD43^+$ $CD24^+$ $BP\text{-}1^+$), D ($B220^+$ $CD43^-$ IgM^-), E ($B220^+$ $CD43^-$ IgM^+), and F ($B220^{high}CD43^-$ IgM^+). Splenic B cells were sorted into transitional 1 (T1) ($B220^+$ $HSA^{high}CD21^-$ $CD23^-$), transitional 2 (T2) ($B220^+$ $HSA^{low}CD21^+$ $CD23^+$), marginal zone (Mz) ($B220^+$ $CD21^+$ $CD23^-$), and follicular (Fo) ($B220^+$ $HSA^{-/low}CD21^{low}CD23^{low}$) B-cell subsets. (B) Reduced size and weight of a $KLHL6^{-/-}$ spleen (left) compared to a normal wild-type spleen (right). A total of three mice were analyzed and they all exhibited the same phenotype. (C) Specific reduction in the percentages of $B220^+$ $CD3^-$ B lymphocytes in spleen and peripheral blood in $KLHL6^{-/-}$ mice. Due to this reduction in B cells, the percentages of $B220^-$ $CD3^+$ T lymphocytes were relatively increased. FACS data are shown for one mouse of each genotype but are representative of 10 mice of each genotype.

MATERIALS AND METHODS

Discovery of KLHL6. Subtractive hybridization between cDNAs from embryonic and adult endothelial cells (tester and driver, respectively) was performed with the PCR-Select Subtraction kit (Clontech). Green fluorescent protein (GFP)-marked endothelial cells were isolated by fluorescence-activated cell sorting (FACS) from embryonic day E15.5 embryos and adult organs (heart, liver, lungs, brain, and skeletal muscle) of Tie2-GFP transgenic mice (18). The subtracted cDNA (i.e., embryo – adult) was further screened with cDNA probes generated from the embryonic and pooled adult endothelial cells. The clones, which hybridized positively with the embryonic probe but negatively with the adult probe, were characterized further. Among these was one novel gene, KLHL6. In situ hybridization with embryonic and adult mouse sections confirmed that this gene was expressed in embryonic blood vessel endothelial cells but not in the vasculature of adult organs (data not shown). In adult mice, instead, we detected high levels of expression in hematopoietic and lymphoid organs (see below and data not shown).

Full-length cDNA was isolated by screening the mouse spleen lambda ZAP II library (Stratagene) using the 0.7-kb cDNA fragment cloned from the subtracted

TABLE 1. Number of splenic B-lineage cells[a]

Genotype	Splenocytes[b] (10^8)	Marginal zone[a] (10^6)	Transitional 1[b] (10^5)	Transitional 2[b] (10^5)	Follicular[b] (10^7)
+/− ($n = 5$)	4.1 ± 1.0	3.1 ± 0.9	14.0 ± 5.8	15.0 ± 3.6	3.8 ± 0.4
−/− ($n = 5$)	2.6 ± 0.3	2.1 ± 0.8	7.0 ± 1.7	6.1 ± 2.5	1.9 ± 0.2

[a] B-lineage cells were defined here by flow cytometry according to the following phenotypes: marginal zone, $B220^+$ CD23 IgM^{high} $CD21^{high}$; transitional 1, $B220^+$ $CD23^-$ IgM^{high} $CD21^{low}$; follicular, $B220^+$ $CD23^+$ IgM^{low} $CD21^{low}$; and transitional 2, $B220^+$ $CD23^+$ IgM^{high} $CD21^{high}$.
[b] *t* test, $P < 0.05$.

TABLE 2. Percentage of Hardy's fractions among B220$^+$ cells in bone marrow

Genotype	Pro-B cells			Pre-B cells (fraction D)	Immature[a] (fraction E)	Mature (fraction F)[a]
	Fraction A	Fraction B	Fraction C			
+/− (n = 3)	1.0 ± 0.3	6.5 ± 1.4	1.1 ± 0.7	37.7 ± 4.8	21.0 ± 1.7	21.0 ± 5.0
−/− (n = 3)	1.1 ± 0.2	6.7 ± 1.2	1.0 ± 0.4	38.8 ± 4.9	32.6 ± 4.2	8.9 ± 1.8

[a] t test, $P < 0.02$.

cDNA library. The analysis of the full-length cDNA revealed that this gene encoded a novel BTB-kelch protein (see Fig. S1A and B in the supplemental material).

Generation of constitutive KLHL6$^{-/-}$ mice. The bacterial artificial chromosome (BAC) genomic clone for the KLHL6 gene was obtained from Research Genetics and the targeting vector was constructed as shown in Fig. S1D in the supplemental material. Electroporation, embryonic stem (ES) cell culture, and Southern blot screening were performed as previously described (28). Chimeric mice were crossed with the CAG:Cre line to remove PGKneo (23). Mice were kept for further studies in CD1, 129/svEms-+Ter$^?$/J, and BALB/c backgrounds. The mouse genotype was analyzed by PCR on genomic DNA using the primers indicated in Fig. S1D in the supplemental material.

Conditional gene targeting of KLHL6. The first exon of the KLHL6 gene was replaced by a fragment containing a floxed first exon followed by an Flp recombination target-flanked PGKneo cassette (see Fig. S3A in the supplemental material). The PGKneo cassette was removed by crossing chimeric mice with hACTB::FLPe.9205 mice (22).

Genetic background and age of the mice. The mice were studied on CD1, 129/svEms-+Ter$^?$/J, and BALB/c backgrounds and the same phenotype was found in all of these backgrounds. The data presented in the manuscript were obtained from the CD1 background mice. The studies were conducted with adult mice at 6 to 10 weeks of age.

Flow cytometry. Splenocytes were isolated by mechanically dissociating mouse spleens through 100-μm nylon mesh (BD Bioscience) in the FACS staining buffer (5% bovine serum albumin–phosphate-buffered saline). Bone marrow cells were collected from femurs and tibias. Antibodies against B220 (RA3-6B2), CD21 (7G6), BP-1 (6C3), CD24 (M1/69), CD43 (S7), CD23 (B3B4), CD40, CXCR5, CD69, and immunoglobulin M (IgM) (II/41) coupled to allophycocyanin, phycoerythrin, fluorescein isothiocyanate, or biotin as appropriate were from BD Bioscience. Streptavidin coupled to peridinin chlorophyll protein (BD Bioscience) was used as the secondary reagent. At least 5×10^5 total cells were analyzed for each experiment. Cells were stained on ice in FACS buffer for 15 min and washed once before analyzing or adding the secondary reagent. In the latter case, cells were stained for another 15 min on ice followed by another washing step. Cells were detected by FACSCalibur or FACScan (Becton Dickinson) flow cytometers and analyzed using CellQuest software.

Footpad assay. Ovalbumin (50 μg/50 μl in PBS) together with 50 μl complete Freund's adjuvant was injected in one footpad of each mouse. The other footpad was injected with PBS as a negative control. Mice were anesthetized 10 days after the injection, and perfused with 4% paraformaldehyde-PBS. Popliteal lymph nodes were dissected, fixed for 4 h at 4°C in 4% paraformaldehyde-PBS, incubated overnight in 18% sucrose at 4°C, and embedded in OCT. Sections (8 μm) were blocked in 3% bovine serum albumin-PBS in room temperature for 1 h and incubated overnight at 4°C with 0.1 μg/ml peanut fluorescein isothiocyanate (FITC)-lectin (Sigma L-7381) in 3% bovine serum albumin-PBS. This lectin staining identifies germinal center B cells in lymph nodes (4). The stained samples were washed, mounted in VECTASHIELD (Vector Laboratories), and examined with an Axioplan microscope (Zeiss) equipped with fluorescence filters. For the analysis of KLHL6 expression in lymph nodes, popliteal lymph nodes were fixed in 4% paraformaldehyde-PBS and paraffin sections were prepared. In situ hybridization was carried out as previously described (24). Germinal center B cells in lymph nodes were measured by staining with antibodies GL7 (BD Bioscience) together with anti-B220.

ELISA for the detection of antiovalbumin antibodies. Each mouse was injected intraperitoneally with 10 μg ovalbumin dissolved in 100 μl PBS together with 100 μl CFA as an emulsion. After 7 and 14 days, mice were boosted with 10 μg ovalbumin dissolved in 100 μl PBS together with 100 μl incomplete Freund's adjuvant. Sera were collected from the mice before the primary ovalbumin injection, 6 days after the first boost, and 6 days after the second boost. Enzyme-linked immunosorbent assay (ELISA) plates were coated overnight at 4°C with 5 μg/ml ovalbumin in 0.05 M carbonate buffer, pH 9.6. On the next day, plates were blocked in 1% bovine serum albumin-PBS, washed three times with PBS–0.05%Tween 20, and loaded with 100 μl of diluted sera (dilutions of 1:10, 1:100, 1:1,000, and 1:10,000 in PBS, in triplicate) and incubated overnight at 4°C. On the following day, the plates were washed three times and incubated for 1 hour at room temperature with horseradish peroxidase-conjugated goat anti-mouse IgG antibody (dilution, 1:3,000). Each well was then washed three times, followed by colorimetric assay with a peroxidase substrate kit (Bio-Rad). Color development was stopped with 2% oxalic acid and the plates were analyzed by a plate reader (405 nm). The optical density at 405 nm was in the linear range between 0 and 1 with the sera diluted to 1:10,000, and these values were used to represent the titers.

In vitro cell proliferation assay. Spleens were removed from the mice and splenocytes were isolated by mechanical dissociation. B cells were purified by depletion of non-B cells using the mouse B-cell isolation kit (Miltenyi Biotec) according to the manufacturer's protocol. The purity of the resulting B-cell fraction (>99%) was confirmed by FACS with anti-B220-phycoerythrin and anti-IgM-FITC antibodies. Approximately 10^6 cells per 96-well plate were seeded in Dulbecco's modified Eagle's medium containing 10% fetal bovine serum, antibiotics, and β-mercaptoethanol. One hour later, the cells were stimulated with lipopolysaccharide, anti-CD40, and anti-IgM for 48 h. Following the stimulation, the cells were incubated with 0.5 μCi [^{3}H]thymidine per well for an additional 20 h. The labeled cells were collected with a cell harvester and the [^{3}H]thymidine incorporation was quantified by liquid scintillation counting.

RT-PCR analysis of KLHL6 expression in B-lymphocyte subsets. B cells were sorted according to the cell surface phenotypes reported by Hardy et al. and by Carsetti and colleagues (5, 11). The cDNAs were synthesized from total RNA isolated from approximately 20,000 cells from each indicated developmental stage. The primers used for KLHL6 were 5′-AGA CCA GGA GAG TGT GCA TGG-3′ and 5′-CGT TGA TGG CAG GAC AAA GAG-3′. The primers for glyceraldehyde-3-phosphate dehydrogenase (GAPDH) were obtained from Clontech. PCR was performed at 94°C (5 minutes), 35 cycles at 94°C (30 seconds), 58°C (30 seconds) 72°C (45 seconds), and 72°C (10 minutes) in the end.

Assays of intracellular free calcium levels in B lymphocytes. Calcium concentrations were measured by the protocol (PP00000011) of the Alliance for Cellular Signaling (www.signaling-gateway.org). B cells isolated by a B-cell isolation kit (Miltenyi Biotec 130-090-862) were resuspended at 5×10^6 cells/ml in SIMDM (Iscove's modified Dulbecco's medium supplied with 2 mM L-glutamine, 55 μM 2-mercaptoethanol, 0.025% Pluronic F-68, and 0.1 mg/ml bovine serum albumin) containing 12 μl/ml Fluo-3 (4 μM) (Molecular Probes) and 12 μl/ml Pluronic F-127 (0.08%) (Molecular Probes). Cells were distributed into six-well ultra-low-attachment plates (Corning) at 2 ml/well. Incubated at 37°C and 5% CO_2 for 30 min, cells were resuspended in fresh SIMDM for another 30 min, pelleted down and resuspended in Hanks' balanced salt solution-bovine serum albumin (Hanks' balanced salt solution supplied with 25 mM HEPES, 1 mg/ml bovine serum albumin, pH 7.4) at 8.3×10^6 cells/ml. The final cell suspension was distributed into 96-well black-walled plates at 90 μl/well and equilibrated in the fluorescence chamber for 5 minutes

Baseline fluorescence was measured for 10 minutes. Ten μl of the F(ab′)$_2$ fragment of goat anti-mouse IgM or anti-CD19 was added to start the stimulation. The fluorescence was measured by Fluoroskan Ascent microplate fluorometer (Thermo-Labsystems) and analyzed by Ascent software (Thermo-Labsystems). For measurements of intracellular calcium levels by FACS, splenocytes were washed with 10% fetal bovine serum-PBS, resuspended at 10^7 cells/ml in loading medium (10% fetal bovine serum-RPMI 1640), and incubated with 5 μg/ml Indo-1 AM (Molecular Probes) for 30 min at 37°C. The cells were stained with phycoerythrin-conjugated anti-B220 monoclonal antibody for 30 min on ice, washed with Hanks' balanced salt solution twice, and resuspended in loading buffer at 10^7 cells/ml. Calcium flux was triggered by adding a F(ab′)$_2$ fragment of goat anti-mouse IgM (Jackson ImmunoResearch Laboratories) or anti-CD19 antibody (MB19-1, BD Biosciences). The calcium fluxes were recorded in real time using a FACSVantage SE instrument (BD Biosciences) and analyzed by FACSDiva (BD Biosciences).

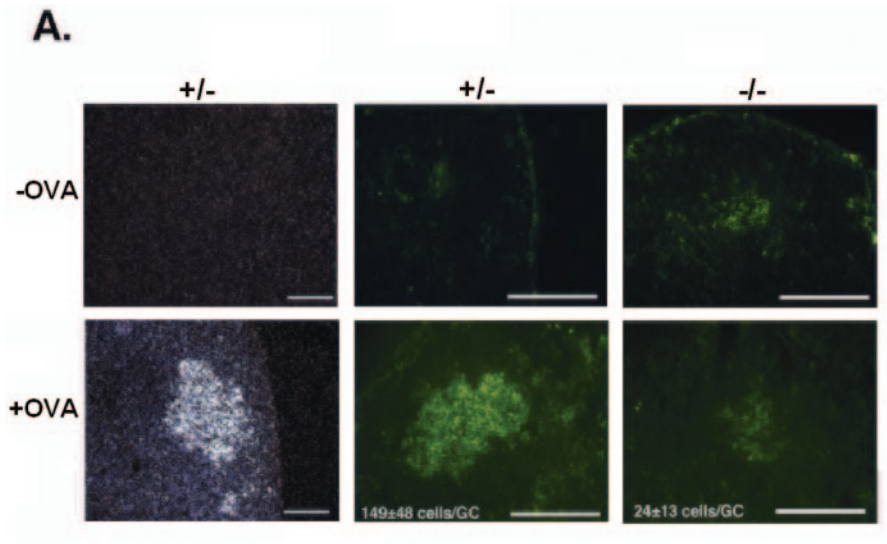

B.

Genotype	-OVA	+OVA	ratio(+OVA/-OVA)
KLHL6$^{+/+}$	3.77± 2.06×10^3	612± 137×10^3	162 ×
KLHL6$^{-/-}$	4.18± 3.36×10^3	203± 76.7×10^3	48.6 ×

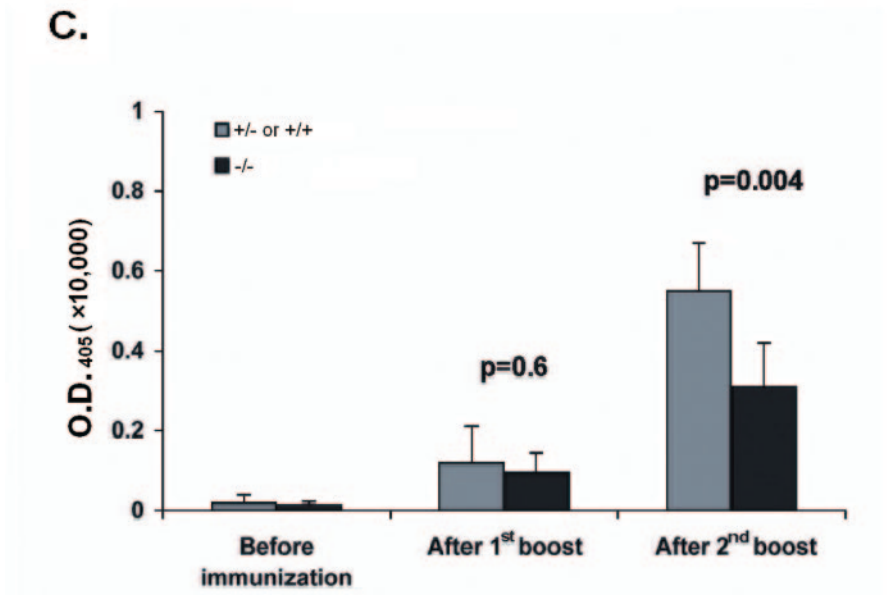

FIG. 2. Impaired germinal center formation and immunoglobulin G memory response in KLHL6-deficient mice. (A) In situ hybridization analysis for expression of KLHL6 in lymph node before (left, top) and after (left, bottom) ovalbumin (OVA) injection. KLHL6 expression was strongly upregulated in germinal centers (GC). Analysis for GC formation by PNA (lectin)-FITC staining revealed large GCs in lymph nodes following ovalbumin injection in heterozygous (and wild-type) mice (middle panels, green). Counting lectin-positive B cells on the sections identified 146 ± 48 cells per GC in heterozygous mice. Formation of GC in lymph nodes was severely compromised in the KLHL6$^{-/-}$ mice (right panels). Counting the FITC-lectin-positive cells in each GC identified only 24 ± 13 cells per GC on the sections in the KLHL6$^{-/-}$ lymph nodes. Two mice were studied for each genotype. Scale bars: 200 μm. (B) Reduced increase of germinal center B lymphocytes in KLHL6$^{-/-}$ lymph nodes. GC B lymphocytes were quantified by FACS analysis using anti-B220 and GL7. Total numbers of B220$^+$ GL7$^+$ GC B cells per lymph node are shown for each genotype. The ratio with ovalbumin/without ovalbumin represents the fold increase in B220$^+$ GL7$^+$ cells. The data are a summary

Inositol 1,4,5-trisphosphate (IP_3) measurement. B cells were resuspended at 2×10^7 cells/ml in RPMI 1640 (supplied with 25 mM HEPES) at 37°C for 30 min. B-cell stimulation was initiated by adding a 100-μl cell suspension into a tube with a 5-μg $F(ab')_2$ fragment of goat anti-mouse IgM, and incubated at 37°C for the indicated periods. The reaction was stopped by adding 100 μl 10% perchloric acid, and the IP_3 level was measured by the D-myoinositol 1,4,5-triphosphate (IP_3) [^{3}H] Biotak assay system (Amersham) according to the manufacturer's protocol.

Immunoprecipitation and immunoblotting. B cells were resuspended in RPMI 1640 (supplied with 25 mM HEPES) at 2×10^7 cells/ml. $F(ab')_2$ fragments of goat anti-mouse IgM were diluted in RPMI 1640 at 30 μg/ml. The cell suspension and the diluted antibody solution were warmed at 37°C for 2 minutes prior to the stimulation. The stimulation was initiated by adding 500 μl of diluted antibody into the 500 μl B-cell suspension (total, 10^7 cells), and incubated at 37°C for the indicated periods. Cells were collected by centrifugation, and lysed using 200 μl ice-cold lysis buffer (Phosphosafe extraction buffer from Novagen) containing the complete protease inhibitor cocktail (Roche), Pefabloc SC (Roche), and 1 mM dithiothreitol on ice for 30 min. Cell lysate (2×10^7 cells for Btk, 10^7 for all the others) was precleared by protein G-agarose (Roche), incubated with the indicated antibody at 4°C for a period ranging from 4 h to overnight, and incubated with protein G-agarose for another 3 h. The protein G-agarose was washed with lysis buffer 3 times, and finally resuspended in loading buffer.

The immunoprecipitated products were heated and subjected to sodium dodecyl sulfate (SDS)-polyacrylamide gel electrophoresis (PAGE) and Western blot analyses. ECL plus (Amersham) was used to detect the signals, and each band was quantified by Storm 860 (Molecular Dynamics). Data were analyzed by ImageQuant software (Molecular Dynamics). The blots were stripped for reprobing with IgG elution buffer (Pierce) according to the user's manual. Anti-phospholipase Cγ2 (PLCγ2)(Q-20), anti-Syk(C-20), anti-Syk(N-19), and anti-phosphotyrosine antibody (PY99) were purchased from Santa Cruz. Anti-Btk polyclonal antibodies were generously provided by Anne Satterthwaite and Owen Witte.

RESULTS

KLHL6 expression in the B-lymphocyte lineage. We had originally identified KLHL6 as a gene that is differentially expressed in embryonic but not in adult vascular endothelial cells. Sequence comparison showed that KLHL6 is a BTB-kelch protein which is highly conserved from zebra fish to humans (see Fig. S1A in the supplemental material). It contains a BTB domain at the N terminus and six kelch repeats at the C terminus (see Fig. S1B and C in the supplemental material). Despite specific expression of KLHL6 in embryonic vasculature, analysis of our KLHL6-deficient mice (see below) revealed apparently normal blood vessel development and function (data not shown).

Others have recently reported that KLHL6 is expressed predominantly in sheep Peyer's patch and human tonsil B lymphocytes (9). To extend this analysis more systematically to various stages of B-cell ontogeny, B-cell progenitors were purified from the bone marrow of normal mice according to Hardy et al. (10). B cells develop from fraction B ($B220^+$ $CD43^+$ $CD24^+$ $BP\text{-}1^-$), via C ($B220^+$ $CD43^+$ $CD24^+$ $BP\text{-}1^+$), D ($B220^+$ $CD43^-$ IgM^-), and E ($B220^+$ $CD43^-$ IgM^+) to F ($B220^{high}$ $CD43^-$ IgM^+). In this order, B to E represent immature and newly generated B cells, while cells in F represent recirculating mature B cells in the bone marrow.

Reverse transcription-PCR (RT-PCR) analysis showed similar expression of KLHL6 throughout B-cell development (Fig. 1A). Splenic B cells were sorted into transitional 1 (T1) ($B220^+$ HSA^{high} $CD21^-$ $CD23^-$), T2 ($B220^+$ HSA^{low} $CD21^+$ $CD23^+$), marginal zone (Mz) ($B220^+$ $CD21^+$ $CD23^-$), and follicular (Fo) ($B220^+$ $HSA^{-/low}$ $CD21^{low}$ $CD23^{low}$) B-cell subsets (6, 16). Again, all of these B-cell populations expressed KLHL6 (Fig. 1A).

Generation of KLHL6-deficient mice. To study the in vivo function of KLHL6, we generated two types of mutant KLHL6 alleles by homologous recombination. The first allele ($KLHL6^{-/-}$) was a constitutive null allele in which the first exon of the KLHL6 gene was deleted. After germ line transmission, the *loxP*-flanked *neo* gene was removed by crossing the mutant mice to a Cre-expressing mouse line (see Fig. S1D to F in the supplemental material and Materials and Methods). $KLHL6^{-/-}$ mice were viable, and all of the null mice were indistinguishable by visual inspection from the wild-type littermates. However, the spleen was significantly smaller in $KLHL6^{-/-}$ compared to wild-type (or heterozygous) littermates (Fig. 1B). The spleen weight was reduced by about 20% (Fig. 1B), and the absolute number of splenocytes was lowered by about 50% (Table 1) comparing $KLHL6^{-/-}$ to wild-type mice.

Flow cytometric analyses revealed a specific reduction in the percentages of the $B220^+$ $CD3^-$ B lymphocytes in the spleen and peripheral blood (Fig. 1C). These phenotypes do not seem to be due to the impaired B-cell survival, based on the fact that the terminal deoxynucleotidyltransferase-mediated dUTP-biotin nick end labeling (TUNEL) staining of the spleen or the flow cytometric analysis of annexin V expression revealed no quantitative differences between wild-type and $KLHL6^{-/-}$ mice (data not shown). However, the possibility that the subtle changes in the B-cell survival and/or cell cycle progression in the mutant mice remains as these standard methods may not detect the relatively rapid B-cell turnover.

Next, we determined the stage in B-cell development at which loss of KLHL6 might affect B-cell development. Frequencies of pro- and pre-B-cell phenotypes in bone marrow were compared between $KLHL6^{-/-}$ and heterozygous littermates (Table 2). No differences were observed for fractions A to D. However, the frequency of cells in fraction E (immature) was increased by about 50%, and the mature population (fraction F) was decreased two- to threefold (Table 2; see also Fig. S2 in the supplemental material). These results indicate that KLHL6 was not required for the early stages of B-cell development. However, loss of KLHL6 affected fractions E and F.

To further resolve the specific distribution of mature B-cell subsets in wild and KLHL6 mutant mice, we measured the absolute numbers of transitional 1 and 2 as well as follicular and marginal zone B cells (each measured phenotype is indicated in the legend for Table 1). T1 and T2 populations were

of values for three mice for each genotype. (C) Compromised antibody production in the $KLHL6^{-/-}$ mice following ovalbumin immunization. In the wild-type and heterozygous mice, antiovalbumin antibody production was significantly increased following the second boost. In contrast, the titer of antiovalbumin antibody in $KLHL6^{-/-}$ mice did not increase as much as that in wild-type/heterozygous mice. The data shown here were obtained from the 1:10,000 dilution of each antiserum. At this dilution, the optical density at 405 nm readings were within the linear range of 0 to 1. A total of three wild-type, six heterozygous, and five homozygous mice were studied. Data shown represent the averages for individual mouse sera. The standard deviation shows the differences among each group.

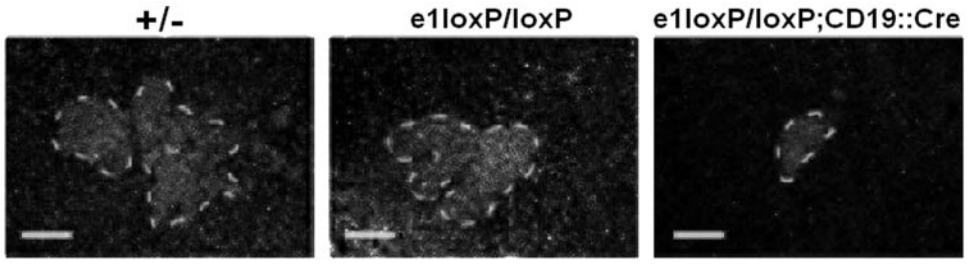

FIG. 3. B-lymphocyte-specific deletion of the KLHL6 gene reproduces the germinal center phenotype of constitutive KLHL6$^{-/-}$ mice. Cryosections of lymph nodes from heterozygous (+/−: left), floxed (e1loxP/loxP: middle), and the B-cell-specific KLHL6 deletion (e1loxP/loxP;CD19::Cre: right) mice after immunization with ovalbumin were stained by FITC-lectin. CD19::Cre-mediated B-cell-specific KLHL6 deletion was sufficient to reproduce the phenotype of impaired GC formation. Scale bar: 100 μm.

reduced two- to threefold, and follicular B cells were reduced by 50%. Although the average number of marginal zone B cells was also smaller in KLHL6$^{-/-}$ mice, the difference was not statistically significant. No differences were detected in peritoneal CD5$^+$ B1 lymphocyte and the CD4$^+$ or CD8$^+$ T-cell populations (data not shown).

Upregulation of KLHL6 expression during germinal center formation, and impaired germinal center formation in mice lacking KLHL6. It has previously been reported that KLHL6 is expressed in sheep Peyer's patch and human tonsil B cells, suggesting that KLHL6 expression may be associated with the germinal center (GC) reaction (9). To test this idea directly, mice were immunized in the footpad with ovalbumin. Wild-type and heterozygous mice exhibited visibly enlarged local lymph nodes. Interestingly, in situ hybridization demonstrated a strong upregulation of KLHL6 expression in the GC (Fig. 2A, left). Thus, KLHL6 expression increases upon antigen-driven GC formation in vivo.

To analyze whether KLHL6 was functionally important for GC formation in vivo, we compared lymph node swelling and the extension of GC formation following ovalbumin immunization in wild-type and KLHL6$^{-/-}$ mice. In contrast to wild-type mice, KLHL6$^{-/-}$ mice showed no comparably enlarged lymph nodes. Formation of enlarged GCs following ovalbumin immunization was detected by lectin (peanut agglutinin [PNA]) staining (Fig. 2A, middle and right). This analysis revealed severely impaired GC formation in KLHL6$^{-/-}$ mice (Fig. 2A, right) compared to wild-type mice (Fig. 2A, middle). The quantification of germinal center B cells by flow cytometry confirmed a smaller increase in B220$^+$ GL7$^+$ germinal center B cells in KLHL6$^{-/-}$ lymph nodes (Fig. 2B).

To determine whether these morphological differences in GC formation correlated with functional alterations, we measured the ovalbumin-specific immunoglobulin G titers before and after primary and secondary immunization with ovalbumin (Fig. 2C). While the primary antibody response was comparable in both wild-type and KLHL6$^{-/-}$ mice, the memory IgG response was clearly reduced in the mutant (Fig. 2C). These data represent the first indication that KLHL6 is functionally important, albeit not essential, for GC formation.

B-lymphocyte-autonomous role of KLHL6 in germinal center formation. The analyses of the expression pattern of KLHL6, and the data on KLHL6$^{-/-}$ mice suggested that KLHL6 plays a role in B cells. However, it remained possible that the function of KLHL6 in non-B lymphocytes indirectly regulated B-lymphocyte development or function. In order to address this issue, we generated and studied a mouse line in which the KLHL6 gene was specifically deleted in B cells. To generate a conditional null allele of KLHL6, the first exon of the KLHL6 gene was flanked by a pair of *loxP* elements in ES cells (see Fig. S3A in the supplemental material). Mutant ES cells were used to establish the "floxed" KLHL6$^{e1+/loxP}$ mouse line (see Fig. S3B in the supplemental material) which was crossed to the CD19::Cre line. The latter has previously been shown to induce B-cell-specific gene deletion in vivo (21). Southern blot analyses of DNA from appropriate F_1 mice demonstrated efficient and specific excision of the first exon of KLHL6 in B but not T cells (see Fig. S3C in the supplemental material).

To distinguish between a B-cell-intrinsic versus a B-cell-extrinsic effect of the loss of KLHL6, B-cell populations and functions were compared in B-cell-specific KLHL6 gene deletion mice, termed KLHL6$^{e1loxP/loxP}$ CD19::Cre, KLHL6$^{+/-}$ and KLHL6$^{e1loxP/loxP}$ control mice. Flow cytometric analyses of bone marrow and spleen showed comparable alterations in B-cell subsets in the KLHL6$^{e1loxP/loxP}$ CD19::Cre mouse line compared to the KLHL6$^{-/-}$ control mice (data not shown). These results indicate that KLHL6 has a cell-autonomous function in B lymphocytes in vivo.

Next, KLHL6$^{e1loxP/loxP}$ CD19::Cre, KLHL6$^{+/-}$ and KLHL6$^{e1loxP/loxP}$ control mice were immunized by ovalbumin injections. In agreement with the data from the constitutive KLHL6$^{-/-}$ mouse, PNA staining revealed compromised GC formation in the lymph nodes of KLHL6$^{e1loxP/loxP}$ CD19::Cre mice (Fig. 3). Quantification by FACS revealed a 228-fold versus 19-fold increase of B220$^+$ GL7$^+$ GC B lymphocytes per lymph node in response to ovalbumin injections in KLHL6$^{e1loxP/lox}$ and KLHL6$^{e1loxP/loxP}$ CD19::Cre mice, respectively. These experiments demonstrate a cell-intrinsic requirement for KLHL6 expression in B cells.

Defects in B-cell antigen receptor signaling in KLHL6$^{-/-}$ mice: role of KLHL6 in BCR-mediated B-cell proliferation. The phenotype of KLHL6-deficient B cells was consistent with an impaired proliferation in response to antigen stimulation. This possibility was tested in an in vitro assay (Fig. 4). Purified B cells were stimulated by lipopolysaccharide, anti-CD40, or anti-IgM. The proliferation was quantified by [^{3}H]thymidine incorporation. No significant differences were detected in lipopolysaccharide- or anti-CD40-stimulated proliferation comparing wild-type and KLHL6$^{-/-}$ B lymphocytes (Fig. 4). In

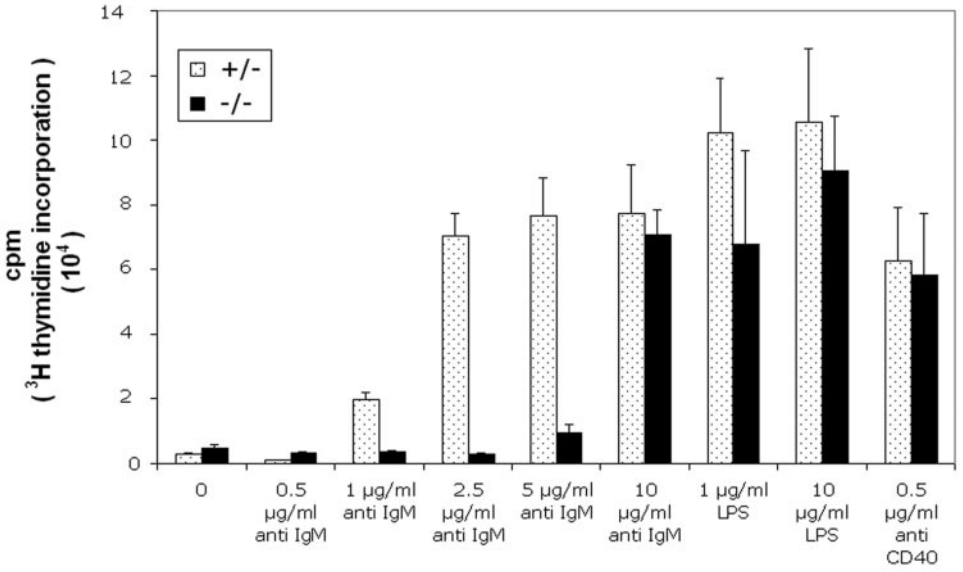

FIG. 4. Impaired B-lymphocyte proliferation in response to anti-IgM stimulation. B lymphocytes from KLHL6$^{-/-}$ spleens exhibited significantly reduced proliferation in response to stimulation by 1, 2.5, and 5 μg/ml anti-IgM antibody. However, at 10 μg/ml anti-IgM, the response was nearly normal, suggesting that KLHL6$^{-/-}$ B lymphocytes were less sensitive to an increasing dose of anti-IgM. No statistically significant differences were detected in response to lipopolysaccharide (LPS) or anti-CD40. A total of four mice of each genotype were analyzed in two independent experiments.

contrast, the proliferation of KLHL6$^{-/-}$ B cells in response to anti-IgM treatment was significantly reduced (Fig. 4). The proliferative response of KLHL6$^{-/-}$ B cells was compromised in response to 1, 2.5, and 5 μg/ml anti-IgM (Fig. 4). However, at 10 μg/ml of anti-IgM, KLHL6$^{-/-}$ B cells proliferated normally (Fig. 4). This difference in the sensitivity to anti-IgM cross-linking was paralleled by the delayed surface expression of the activation marker CD69 in response to increasing doses of anti-IgM (see Fig. S4 in the supplemental material) (25). These results suggests that KLHL6$^{-/-}$ B cells are less sensitive to anti-IgM but not lipopolysaccharide or anti-CD40 stimulation, pointing to a role for KLHL6 in the antigen-stimulated proliferative B-cell response.

B-cell receptor signaling in KLHL6$^{-/-}$ mice. To gain information as to whether BCR-signaling pathways were affected by the loss of KLHL6, signal transduction downstream of the BCR (7, 15, 20) was compared in wild-type and KLHL6$^{-/-}$ B cells. As a population, KLHL6$^{-/-}$ B cells showed a markedly reduced increase in the level of intracellular Ca^{2+} in response to anti-IgM stimulation compared to wild-type B cells (Fig. 5A). To determine the frequencies of B cells which exhibited such low Ca^{2+} response, we measured stimulation-dependent changes in intracellular calcium levels in individual cells by FACS. This analysis demonstrated an impaired anti-IgM response in a substantial fraction of KLHL6$^{-/-}$ B cells (Fig. 5B).

Detailed biochemical analyses showed a corresponding reduction of IP_3 production (Fig. 5C) and partial failure of the activation of PLCγ2 and Btk tyrosine kinase, but not of Syk tyrosine kinase (Fig. 5D to I). These biochemical analyses suggested that KLHL6 was involved in antigen-stimulated B-cell activation via Btk-mediated BCR signaling pathways. However, compared to the reduction in B-cell proliferation, the measurable defects in BCR signaling were rather mild.

DISCUSSION

Herein, we report a physiological function within the immune system for KLHL6, a highly conserved BTB-kelch protein. KLHL6$^{-/-}$ mice exhibited several defects in B-lineage cells. KLHL6 was expressed throughout all stages of B-cell development but analysis of KLHL6$^{-/-}$ mice revealed defects only in mature B-cell subsets. Specifically, we noted the following key findings. (i) Pro- and pre-B-cell development proceeded independently from KLHL6. (ii) Several subsets of peripheral B cells were reduced in number. (iii) Antigen-driven expansion of germinal center B cells was reduced. (iv) Antiovalbumin IgG titers were reduced following the second immunization. (v) BCR signaling was impaired in KLHL6$^{-/-}$ B cells, leading to reductions in proliferation, Ca^{2+} response, and PLCγ2 activation in vitro. Finally, we demonstrate a B-cell-autonomous function of KLHL6.

The most striking aspect of the mutant phenotype reported here was the failure of KLHL6$^{-/-}$ mice to mount a full GC reaction in vivo. In a previous screen for genes differentially expressed in B cells undergoing immunoglobulin hypermutation, two genes have emerged as interesting candidates: the RING finger ubiquitin ligase Deltex-1, and KLHL6 (9). A role for Deltex-1 in the immune system has recently been excluded based on a detailed analysis of Deltex-1-deficient mice (27). With regard to KLHL6, expression of this gene in lymphoid tissues (9), specifically in all stages of B-cell development (Fig. 1), suggested a role in B cells. Moreover, expression of KLHL6 in sheep Peyer's patch and human tonsil B cells (9), together with the fact that KLHL6 expression was a strong histological marker of the GC (Fig. 2), suggested a functional relevance of KLHL6 expression for GC B cells. However, until now, defin-

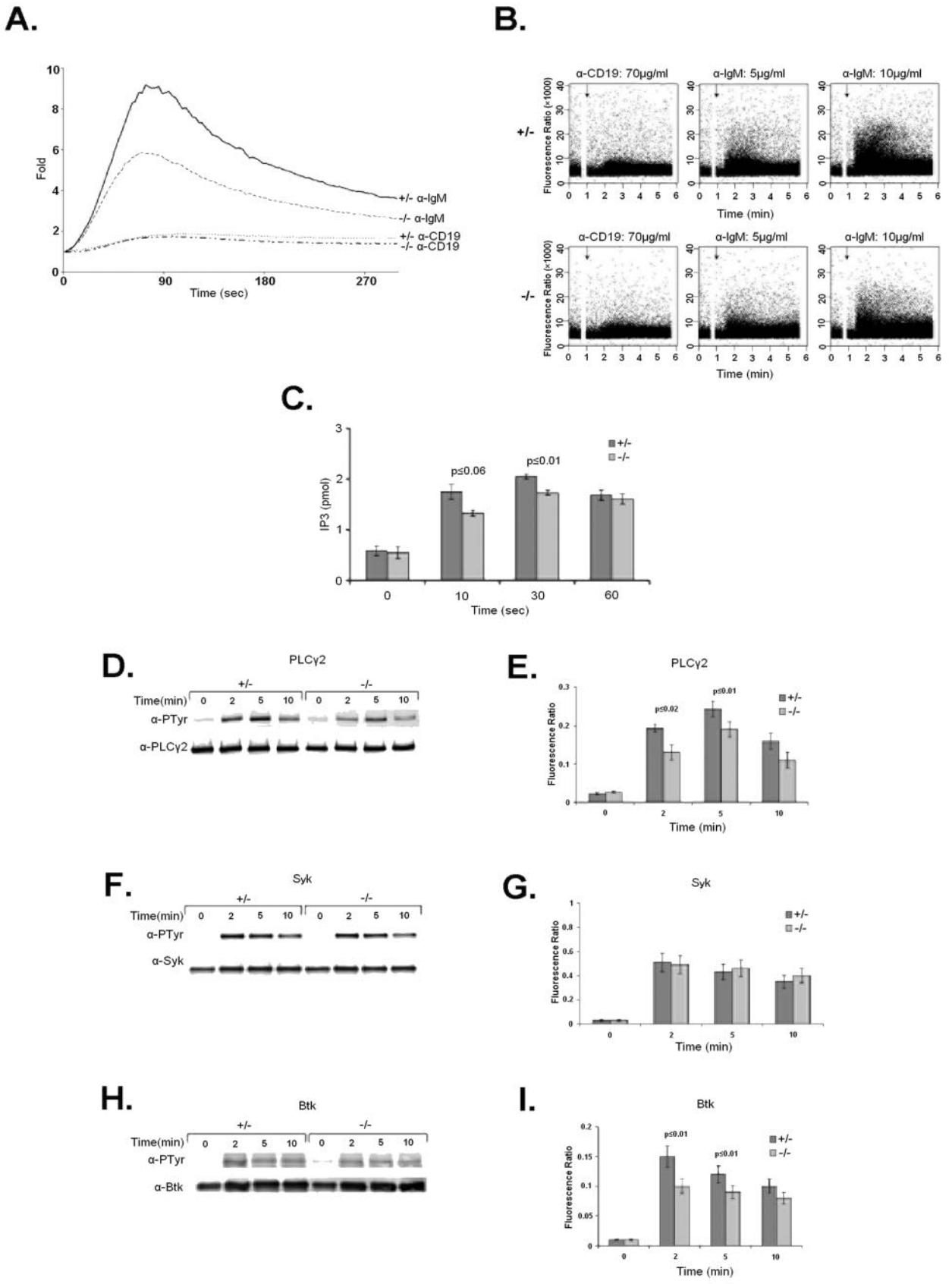
A.
Fold
Time (sec)
+/- α-IgM
-/- α-IgM
+/- α-CD19
-/- α-CD19
B.
α-CD19: 70μg/ml
α-IgM: 5μg/ml
α-IgM: 10μg/ml
+/-
-/-
Fluorescence Ratio (x1000)
Time (min)
C.
IP3 (pmol)
p≤0.06
p≤0.01
+/-
-/-
Time (sec)
D.
PLCγ2
+/-
-/-
Time(min)
α-PTyr
α-PLCγ2
E.
PLCγ2
Fluorescence Ratio
p≤0.02
p≤0.01
Time (min)
F.
Syk
α-PTyr
α-Syk
G.
Syk
Fluorescence Ratio
Time (min)
H.
Btk
α-PTyr
α-Btk
I.
Btk
Fluorescence Ratio
p≤0.01
Time (min)

itive information on the role of KLHL6 has been lacking because mutant mice lacking this gene have not been reported.

The in vivo data on the GC phenotype and the B-cell numbers correlated with the impaired B-lymphocyte proliferation and compromised calcium flux in response to anti-IgM stimulation in vitro. The flow cytometric calcium flux analysis was done by gating on $CD19^+$ B cells. Therefore, we cannot draw conclusions regarding the ability of rare B-cell subpopulations such as transitional or marginal zone B cells to show calcium responses.

Continuous expression of a fully signaling competent BCR is essential for the maintenance of the peripheral B-lymphocyte pool (14). Hence, the involvement of KLHL6 in BCR signaling could be important for antigen-stimulated B-lymphocyte proliferation. Along this line, in addition to GC B cells, the numbers of other B-cell subsets (T1, T2, and follicular B cells) were also quantitatively affected by the loss of KLHL6, suggesting a role of this gene in the generation and/or maintenance of normal B-cell compartments in vivo.

Although we do not have data to pinpoint exactly how KLHL6 is involved in the BCR signaling, a few possibilities can be proposed. It is possible that KLHL6 can serve as an adaptor for cullin 3 ubiquitin ligases for a putative substrate that affects BCR signaling. Another possibility is that KLHL6 is involved in regulating the cytoskeletal remodeling of B lymphocytes. It has been shown that many BTB-kelch proteins are important for normal cytoskeletal organization and remodeling (1). The normal cytoskeletal organization/remodeling and its related signaling and cell biological events are important for PLCγ2 signaling (3, 17). Thus, KLHL6 may be important for cytoskeletal organization, and deficiency of this KLHL6 function could result in impaired PLCγ2 signaling. It is conceivable that these aspects of impaired BCR signaling contribute to the underlying defects in B-cell function. However, the differences in Ca^{2+} influx, IP3 production, and the activation of Btk and PLCγ2 between the wild-type and $KLHL6^{-/-}$ B lymphocytes were marginal, albeit statistically significant. In contrast, the proliferation of B lymphocytes was severely compromised. This discrepancy may indicate that the observed alterations in BCR signal transduction do not fully reflect the key mechanism underlying the role of KLHL6 in B cells. The exact mechanism(s) remains to be determined.

KLHL6 is the third member of mammalian BTB-kelch proteins whose physiological function has been directly demonstrated. The other two are Keap1 and KLHL10 (30, 33). These studies showed rather diverse physiological functions of BTB-kelch proteins. Is there a unifying molecular and biochemical mechanism underlying these diverse functions of BTB-kelch proteins? Some of the BTB-kelch proteins, including Keap1, are associated with actin in cells (1). We generated an epitope-tagged KLHL6 protein which we expressed in cultured cells. This protein was mostly localized in the perinuclear region, but no consistent colocalization with actin was detected (data not shown). A new protein motif, the BACK (for BTB and C-terminal Kelch) domain, is present in most BTB-kelch proteins (26). Our in silico analysis of Keap1, KLHL10, and KLHL6 sequences showed that they all contain the BACK domain. However, the relevance of this novel domain to the apparent diverse physiological functions among BTB-kelch proteins remains unknown.

Our results show that KLHL6 is not essential for GC formation but that KLHL6 deficiency results in impaired GC formation in peripheral lymph nodes (Fig. 2 and 3). This GC phenotype may be a consequence of the lowered threshold of antigen-driven BCR signaling leading to reduced B-lymphocyte proliferation in the GC. However, it is also possible that KLHL6 possesses a yet-unidentified function in B cells that is crucial for normal GC formation. We have partially tested this possibility by analyses of expression of CD40 and CXCR5, known to play a critical role in GC formation (see Fig. S5 in the supplemental material). This analysis showed a normal level of expression of CD40 and CXCR5 in $KLHL6^{-/-}$ B lymphocytes, suggesting that the functional role of KLHL6 in GC formation occurs independently of CD40 or CXCR5.

Collectively, this first report has demonstrated a role for KLHL6 in GCs but has also raised many other questions which shall be addressed in detailed future experiments. Because immunoglobulin isotype switching and somatic hypermutation of immunoglobulin hypervariable regions represent important immunological events in GCs, it should be interesting to compare wild-type and $KLHL6^{-/-}$ mice for their capacity to mount these responses.

ACKNOWLEDGMENTS

We thank Junko Kuno, Tosh Motoike, Patricia Cobo, Charlene Case, and UTSW core facilities for their technical assistance. We also

FIG. 5. Changes in B-cell antigen receptor signaling in $KLHL6^{-/-}$ B lymphocytes. (A) Impaired increase in intracellular free calcium in $KLHL6^{-/-}$ B cells in response to BCR stimulation. Purified B cells were loaded with Fluo-3 and stimulated with $F(ab')_2$ goat anti-mouse IgM (5 μg/ml) or anti-CD19 (5 μg/ml) at time zero. The fluorescence of Fluo-3 was measured with filters for excitation at 485 nm and for emission at 538 nm. Fold increase is shown as the ratio of internal Ca^{2+} concentration ($[Ca^{2+}]_i$) levels (after/before the stimulation). The results are representative of three independent experiments. (B) The BCR-stimulated Ca^{2+} flux is impaired in individual $KLHL6^{-/-}$ B lymphocytes. The Ca^{2+} fluxes were analyzed by FACS. Splenocytes were loaded with Indo-1 and stained with phycoerythrin-conjugated anti-B220 monoclonal antibody. $B220^+$ B lymphocytes from $KLHL^{+/-}$ (top) and $KLHL6^{-/-}$ (bottom) mice were examined for the $[Ca^{2+}]_i$ levels by adding $F(ab')_2$ goat anti-mouse IgM, or anti-CD19 at the indicated time points (arrows). The $[Ca^{2+}]_i$ was determined as the ratio of bound (395 nm) to unbound (530 nm) Indo-1. The results are representative of three independent experiments. (C) Impaired BCR-stimulated increase of IP_3 in $KLHL6^{-/-}$ B cells. B cells were stimulated with 50 μg/ml $F(ab')_2$ goat anti-mouse IgM for the indicated times, and the IP_3 levels were measured. The results were expressed in picomoles of IP_3 per 2×10^6 cells ($n = 4$, mean ± standard deviation). (D to I) BCR-stimulated activation of PLCγ2 (D), Syk (F), and Btk (H). Typical immunoprecipitation/Western blot results for PLCγ2 (D), Syk (F), and Btk (H) are shown. The top lanes show each of the tyrosine-phosphorylated protein bands. The bottom lanes show each of the total immunoprecipitated protein bands. The signal on each Western blot was quantified on a Storm 860 instrument, and the data were analyzed by ImageQuant software. The results are expressed as fluorescence ratios of the phosphotyrosine-containing protein to the total protein levels for PLCγ2 (E) ($n = 4$), for Syk (G) ($n = 6$), and for Btk (I) ($n = 4$). Bars show mean ± standard deviation. *P* values are indicated.

thank Shmuel Muallem, Richard Scheuermann, and Didier Stainier for their help on IP_3 analysis, BCR signaling analyses, and zebra fish gene analysis, respectively, and A. Satterthweite and O. Witte for anti-Btk antibody. We express our appreciation to Alison Kuremsky and Ziming Zou for editing the manuscript and figure preparation, respectively.

J.K. was supported in part by Deutsche Forschungsgemeinschaft (KR1887/2-1). This work was initially funded by the Sponsored Research Agreement with Pharmacia and later supported by the NIH (T.N.S.). H.-R.R. was supported by DFG (SFB-497-B5).

We declare that we have no competing financial interests.

REFERENCES

1. **Adams, J., R. Kelso, and L. Cooley.** 2000. The kelch repeat superfamily of proteins: propellers of cell function. Trends Cell Biol. **10:**17–24.
2. **Bomont, P., L. Cavalier, F. Blondeau, C. Ben Hamida, S. Belal, M. Tazir, E. Demir, H. Topaloglu, R. Korinthenberg, B. Tuysuz, P. Landrieu, F. Hentati, and M. Koenig.** 2000. The gene encoding gigaxonin, a new member of the cytoskeletal BTB/kelch repeat family, is mutated in giant axonal neuropathy. Nat. Genet. **26:**370–374.
3. **Bunnell, S. C., V. Kapoor, R. P. Trible, W. Zhang, and L. E. Samelson.** 2001. Dynamic actin polymerization drives T cell receptor-induced spreading: a role for the signal transduction adaptor LAT. Immunity **14:**315–329.
4. **Butcher, E. C., R. V. Rouse, R. L. Coffman, C. N. Nottenburg, R. R. Hardy, and I. L. Weissman.** 1982. Surface phenotype of Peyer's patch germinal center cells: implications for the role of germinal centers in B-cell differentiation. J. Immunol. **129:**2698–2707.
5. **Carsetti, R.** 2004. Characterization of B-cell maturation in the peripheral immune system. Methods Mol. Biol. **271:**25–35.
6. **Carsetti, R., M. M. Rosado, and H. Wardmann.** 2004. Peripheral development of B cells in mouse and man. Immunol. Rev. **197:**179–191.
7. **Gauld, S. B., J. M. Dal Porto, and J. C. Cambier.** 2002. B-cell antigen receptor signaling: roles in cell development and disease. Science **296:**1641–1642.
8. **Geyer, R., S. Wee, S. Anderson, J. Yates, and D. A. Wolf.** 2003. BTB/POZ domain proteins are putative substrate adaptors for cullin 3 ubiquitin ligases. Mol. Cell **12:**783–790.
9. **Gupta-Rossi, N., S. Storck, P. J. Griebel, C. A. Reynaud, J. C. Weill, and A. Dahan.** 2003. Specific over-expression of deltex and a new Kelch-like protein in human germinal center B cells. Mol. Immunol. **39:**791–799.
10. **Hardy, R. R., C. E. Carmack, S. A. Shinton, J. D. Kemp, and K. Hayakawa.** 1991. Resolution and characterization of pro-B and pre-pro-B-cell stages in normal mouse bone marrow. J. Exp. Med. **173:**1213–1225.
11. **Hardy, R. R., and S. A. Shinton.** 2004. Characterization of B lymphopoiesis in mouse bone marrow and spleen. Methods Mol. Biol. **271:**1–24.
12. **Itoh, K., N. Wakabayashi, Y. Katoh, T. Ishii, K. Igarashi, J. D. Engel, and M. Yamamoto.** 1999. Keap1 represses nuclear activation of antioxidant responsive elements by Nrf2 through binding to the amino-terminal Neh2 domain. Genes Dev. **13:**76–86.
13. **Kelso, R. J., A. M. Hudson, and L. Cooley.** 2002. Drosophila Kelch regulates actin organization via Src64-dependent tyrosine phosphorylation. J. Cell Biol. **156:**703–713.
14. **Kraus, M., M. B. Alimzhanov, N. Rajewsky, and K. Rajewsky.** 2004. Survival of resting mature B lymphocytes depends on BCR signaling via the Igalpha/beta heterodimer. Cell **117:**787–800.
15. **Kurosaki, T.** 1999. Genetic analysis of B-cell antigen receptor signaling. Annu. Rev. Immunol. **17:**555–592.
16. **Loder, F., B. Mutschler, R. J. Ray, C. J. Paige, P. Sideras, R. Torres, M. C. Lamers, and R. Carsetti.** 1999. B-cell development in the spleen takes place in discrete steps and is determined by the quality of B-cell receptor-derived signals. J. Exp. Med. **190:**75–89.
17. **McNamee, H. P., D. E. Ingber, and M. A. Schwartz.** 1993. Adhesion to fibronectin stimulates inositol lipid synthesis and enhances PDGF-induced inositol lipid breakdown. J. Cell Biol. **121:**673–678.
18. **Motoike, T., S. Loughna, E. Perens, B. L. Roman, W. Liao, T. C. Chau, C. D. Richardson, T. Kawate, J. Kuno, B. M. Weinstein, D. Y. Stainier, and T. N. Sato.** 2000. Universal GFP reporter for the study of vascular development. Genesis **28:**75–81.
19. **Pintard, L., J. H. Willis, A. Willems, J. L. Johnson, M. Srayko, T. Kurz, S. Glaser, P. E. Mains, M. Tyers, B. Bowerman, and M. Peter.** 2003. The BTB protein MEL-26 is a substrate-specific adaptor of the CUL-3 ubiquitin-ligase. Nature **425:**311–316.
20. **Reth, M., and J. Wienands.** 1997. Initiation and processing of signals from the B-cell antigen receptor. Annu. Rev. Immunol. **15:**453–479.
21. **Rickert, R. C., J. Roes, and K. Rajewsky.** 1997. B-lymphocyte-specific, Cre-mediated mutagenesis in mice. Nucleic Acids Res. **25:**1317–1318.
22. **Rodriguez, C. I., F. Buchholz, J. Galloway, R. Sequerra, J. Kasper, R. Ayala, A. F. Stewart, and S. M. Dymecki.** 2000. High-efficiency deleter mice show that FLPe is an alternative to Cre-loxP. Nat. Genet. **25:**139–140.
23. **Sakai, K., and J. Miyazaki.** 1997. A transgenic mouse line that retains Cre recombinase activity in mature oocytes irrespective of the cre transgene transmission. Biochem. Biophys. Res. Commun. **237:**318–324.
24. **Sato, T. N., and S. Bartunkova.** 2000. Analysis of embryonic vascular morphogenesis. Methods Mol. Biol. **137:**223–233.
25. **Sohn, H. W., H. Gu, and S. K. Pierce.** 2003. Cbl-b negatively regulates B-cell antigen receptor signaling in mature B cells through ubiquitination of the tyrosine kinase Syk. J. Exp. Med. **197:**1511–1524.
26. **Stogios, P. J., and G. G. Prive.** 2004. The BACK domain in BTB-kelch proteins. Trends Biochem. Sci. **29:**634–637.
27. **Storck, S., F. Delbos, N. Stadler, C. Thirion-Delalande, F. Bernex, C. Verthuy, P. Ferrier, J. C. Weill, and C. A. Reynaud.** 2005. Normal immune system development in mice lacking the Deltex-1 RING finger domain. Mol. Cell. Biol. **25:**1437–1445.
28. **Swiatek, P. J., and T. Gridley.** 1993. Perinatal lethality and defects in hindbrain development in mice homozygous for a targeted mutation of the zinc finger gene Krox20. Genes Dev. **7:**2071–2084.
29. **Timmerman, V., P. De Jonghe, and C. Van Broeckhoven.** 2000. Of giant axons and curly hair. Nat. Genet. **26:**254–255.
30. **Wakabayashi, N., K. Itoh, J. Wakabayashi, H. Motohashi, S. Noda, S. Takahashi, S. Imakado, T. Kotsuji, F. Otsuka, D. R. Roop, T. Harada, J. D. Engel, and M. Yamamoto.** 2003. Keap1-null mutation leads to postnatal lethality due to constitutive Nrf2 activation. Nat. Genet. **35:**238–245.
31. **Xu, L., Y. Wei, J. Reboul, P. Vaglio, T. H. Shin, M. Vidal, S. J. Elledge, and J. W. Harper.** 2003. BTB proteins are substrate-specific adaptors in an SCF-like modular ubiquitin ligase containing CUL-3. Nature **425:**316–321.
32. **Xue, F., and L. Cooley.** 1993. kelch encodes a component of intercellular bridges in Drosophila egg chambers. Cell **72:**681–693.
33. **Yan, W., L. Ma, K. H. Burns, and M. M. Matzuk.** 2004. Haploinsufficiency of kelch-like protein homolog 10 causes infertility in male mice. Proc. Natl. Acad. Sci. USA **101:**7793–7798.